Research Paper
https://doi.org/10.7733/jnfcwt.2020.18.S.75

Safety Assessment on Long-term Radiological Impact of the Improved KAERI Reference Disposal System (the KRS$^+$)

Heejae Ju*, In-Young Kim, Youn-Myoung Lee, Jung-Woo Kim, Yongsoo Hwang, Heui-joo Choi, and Dong-Keun Cho
Korea Atomic Energy Research Institute, 111, Daedeok-daero 989beon-gil, Yuseong-gu, Daejeon, Republic of Korea

(Received August 25, 2020 / Revised September 17, 2020 / Approved October 21, 2020)

The Korea Atomic Energy Research Institute (KAERI) has developed geological repository systems for the disposal of high-level wastes and spent nuclear fuels (SNFs) in South Korea. The purpose of the most recently developed system, the improved KAERI Reference Disposal System Plus (KRS$^+$), is to dispose of all SNFs in Korea with improved disposal area efficiency. In this paper, a system-level safety assessment model for the KRS$^+$ is presented with long-term assessment results. A system-level model is used to evaluate the overall performance of the disposal system rather than simulating a single component. Because a repository site in Korea has yet to be selected, a conceptual model is used to describe the proposed disposal system. Some uncertain parameters are incorporated into the model for the future site selection process. These parameters include options for a fractured pathway in a geosphere, parameters for radionuclide migration, and repository design dimensions. Two types of SNF, PULS7 from a pressurized water reactor and Canada Deuterium Uranium from a heavy water reactor, were selected as a reference inventory considering the future cumulative stock of SNFs in Korea. The highest peak radiological dose to a representative public was estimated to be 8.19×10^{-4} mSv·yr^{-1}, primarily from ^{129}I. The proposed KRS$^+$ design is expected to have a high safety margin that is on the order of two times lower than the dose limit criterion of 0.1 mSv·yr^{-1}.

Keywords: Spent nuclear fuel, Disposal system, Geological repository, Safety assessment, KAERI reference system

*Corresponding Author.
Heejae Ju, Korea Atomic Energy Research Institute, E-mail: heejaeju@kaeri.re.kr, Tel: +82-42-866-6418

ORCID

Heejae Ju	http://orcid.org/0000-0002-3879-8770	In-Young Kim	http://orcid.org/0000-0003-1445-0398
Youn-Myoung Lee	http://orcid.org/0000-0003-0317-6784	Jung-Woo Kim	http://orcid.org/0000-0001-6896-471X
Yongsoo Hwang	http://orcid.org/0000-0003-0858-3717	Heui-joo Choi	http://orcid.org/0000-0001-9253-7697
Dong-Keun Cho	http://orcid.org/0000-0003-4152-8605		

1. Introduction

Since 1997, the Korea Atomic Energy Research Institute (KAERI) has developed geological repository systems to dispose of high-level wastes (HLWs) and spent nuclear fuels (SNFs) generated in the Republic of Korea. The proposed design has been modified following reference characteristics of radioactive wastes. The reference characteristics include burnup of SNF, radionuclides inventory, radioactivity, heat generation, cooling time, and geometry of wastes. The first generation repository design called KAERI Reference disposal System (KRS) aimed to dispose of Korean Standard Fuel Assembly (KSFA) type SNF with the average burnup of 45 GWD/tU and SNFs from CANada Deuterium Uranium (CANDU) reactors with the average burnup of 8.1 GWD/tU [1]. Much of the KRS design was similar to the Swedish KBS-3V repository, whose host rock is a deep crystalline rock below 500 m [19]. The next generation repository, called the Advanced KRS (A-KRS), was designed for radioactive wastes originated from pyro-processed SNFs, called PLUS7 (advanced nuclear fuel assembly for Korean standard nuclear reactor), with the average burnup of 55 GWD/tU [1].

After the Basic Plan for Management of High-Level Waste (HLW) recommended two options for SNFs in Korea, a consensus has been made to update the previous repository design to dispose of SNFs in Korea directly. Unlike 1997 when the KAERI first proposed the direct disposal system called the KRS design, the burnup and the cooling time of accumulative SNFs inventory in Korea have increased. Accordingly, Cho et al. suggested the reference SNFs from the pressurized water reactor (PWR) be PLUS7 rather than KSFA, which was the reference SNFs in the previous KRS design [2]. In compliance with the suggested reference SNFs, KAERI has modified the KRS design since 2018. The modified KRS called the KRS plus (KRS$^+$), is designed to accommodate the reference PLUS7 SNFs and CANDU SNFs. The cooling time for each type of SNF is 45 years and 30 years, respectively. Details on selecting reference SNF characteristics for KRS$^+$ are referred elsewhere [2, 7].

In addition to the update in the reference SNFs inventory, modification has been made for the repository design of CANDU SNFs. In the previous KRS design, an engineered barrier system (EBS) of CANDU SNFs was almost the same as the EBS of PWR SNF. The EBS of the KRS consists of a repository tunnel with vertical disposition boreholes filled with buffer material. However, decay heat from CANDU SNFs is lower than PWR SNFs, so the same EBS design application is inefficient. For this reason, the KRS$^+$ disposes of CANDU SNF along with the repository tunnel in a horizontal direction so that the efficiency in the repository area can be improved. Details on the design modification on the CANDU repository are explained in Section 2.1 of this paper and are referred elsewhere [8].

This study aims to evaluate the performance of the KRS$^+$, thereby confirming the long-term safety of the proposed design before the detailed site selection process begins. This performance evaluation before the site selection falls into the preliminary safety assessment process. The safety assessment is a continuous iterative process giving feedback to the repository design while knowledge for potential repository site is updated as site selection proceeds. Accordingly, the repository design would be modified to ensure a high safety margin. Therefore, this paper covers the developing a system-level safety assessment model for and evaluating the radiological impact of the KRS$^+$ design concept. Here, the system-level means that the model can consider repository performances as a whole system. The model is developed based on an insight conceptual model for the disposal system using the Transport module in GoldSim software [5]. Uncertainty in the model due to the absence of a disposal site in Korea is compensated through some conservative assumptions. Finally, the safety assessment result is compared with the international radiological dose limit criteria.

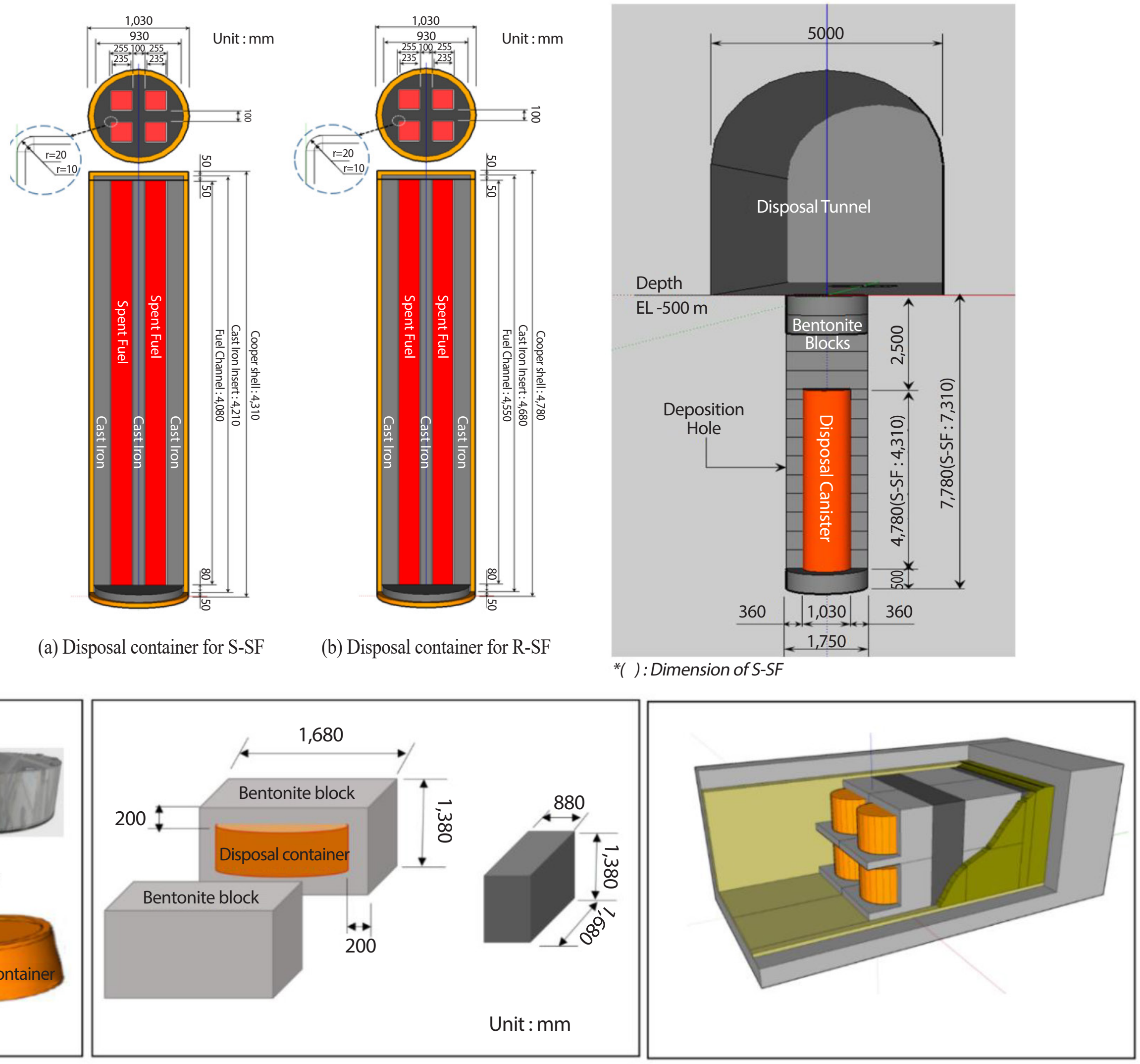

(a) Disposal container for S-SF (b) Disposal container for R-SF

(a) Disposal container (b) Buffer box & Dense Backfill (c) Concept of the NWMO type Horizontal disposal

Fig. 1. The EBS design of PWR-V for PLUS7 SNF (top) and CANDU-H for CANDU SNF (bottom) [8].

2. Methodology

2.1 Repository System of KRS+

In this study, two types of reference SNFs for KRS+ are considered: PLUS7 SNFs with the burnup of 55 GWD/tU, and CANDU SNFs with 8.1 GWD/tU. The cooling time of SNF is assumed to be 45 years for PWR and 30 years for CANDU, respectively. Detail background for selecting reference SNF of KRS+ is referred from [2, 7]. Each reference SNF has a different EBS concept (see Fig. 1). The EBS concept of PLUS7, called PWR-V type, is a typical tunnel repository with vertical deposition boreholes. Like the Swedish KBS3-V concept [19], a copper disposal canister containing four fuel assemblies is emplaced in the vertical deposition hole and sealed with high-density bentonite. On the other hand, in the case of CANDU, the KRS+ adopts a horizontal two-layered buffer box concept (CANDU-H type). The buffer box consists of bentonite blocks surrounding a cooper disposal canister with a single CANDU basket. The buffer boxes are emplaced in two by two layers along a disposal tunnel.

The KRS+ is designed considering deep crystalline host rock. The geological repository concept hosted by crystalline rock has already been considered in various countries [12, 15, 19]. However, socio-geographical conditions for a final SNFs repository in Korea are unique. Most countries whose host rock for the geological repository are hard crystalline have extensive land areas and low population density. On the other hand, a limited land area with high population density Korea is a critical constraint against the scientific site selection process [6]. Japan is also in a similar situation. For this reason, the Nuclear Waste Management Organization of Japan (NUMO) has adopted the Structured Approach to tailor future repository design considering the site condition of unpreferable [12, 13]. Likewise, the design approach of KRS+ is to gain enough safety margin by relying much on a sound engineered barrier system (EBS) rather than relying on a natural barrier (host rock). Applying this approach, the KRS+ aims to achieve an efficient layout with a small footprint while a high safety margin is maintained in any potential circumstances.

2.2 Conceptual Model

As mentioned in Section 2.1, the design approach of the KRS+ is to keep EBS in high performance, thereby lessening the system reliance on the natural barrier. For this reason, the developed model adopts conservatism in the natural barrier so that flexible site selection would be possible in the future. Figure 2 depicts a conceptual mass transport pathway in the developed compartment model for the disposal system of the KRS+.

The degradation of the UO_2 SNF matrix is a critical process that determines radionuclides' release after canister failure. In the model, three modes of degradation process can be considered: fixed fractional dissolution, congruent dissolution, and instantaneous release. The fixed fractional dissolution assumes that a specified fraction of radionuclides is released to groundwater annually. This is quite a conservative assumption because the UO_2 matrix consisting of the SNF rod is very stable under reducing condition, thereby inhibiting the release of radionuclides from the matrix. In this context, the congruent dissolution model where the solubility limit of UO_2 determines the release of radionuclides is more realistic. Some fission products exist in the gap between the fuel rod and cladding as a gas state. Unlike radionuclides within a waste matrix, they instantaneously dissolve into groundwater and start release. This mode of degradation process is called instantaneous release. After the instantaneous release, the concentrations of released radionuclides are controlled by solubility limits.

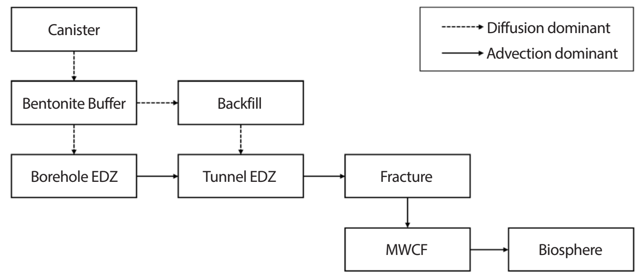

Fig. 2. The schematic diagram for the conceptual model of the KRS+.

In this study, the model assumes that safety functions of each component constituting the EBS are not disturbed. This implies that diffusive mass flux is dominant in the EBS for a period of the safety assessment (dashed arrows in Fig. 2). The components of EBS include disposal canister, buffer, and backfill. Details on the safety functions of each component are referred to elsewhere [8]. Alternative scenarios accompanying events that possibly impair the functions of EBS components are not considered in this study.

The model assumes groundwater flow in an excavated disturbed zone (EDZ) surrounding disposition holes and disposal tunnels. In the EDZ, advective flow is defined by Eq. 1, where Q is the volumetric flow rate in the EDZ [$m^3 \cdot yr^{-1}$], v_D the Darcy velocity perpendicular to repository plane [$m \cdot yr^{-1}$], and A_{EDZ} the area of the EDZ perpendicular to the Darcy velocity [m^3].

$$Q = v_D \cdot A_{EDZ} \tag{1}$$

The model assumes a single fracture intersecting the upper side of the disposal tunnel so that released radionuclides migrate through the fracture and reach a main water-conducting feature (MWCF). The MWCF is a rock far from the repository where numerous fractures compose a network, thereby enabling a large volume of groundwater flow. It should be noted that this assumption is quite conservative because the existence of fracture intersecting the tunnel will be excluded during the site selection and construction process. A more realistic assumption would be that a porous geosphere with low permeability is between the repository and the fractured geosphere. Nevertheless, the conceptual model gives no credit to the porous geosphere to ensure a high safety margin for the designed EBS.

The mass transport in a fracture with an average aperture of $2b$ is given by Eq. 2, where C_i is the concentration of nuclide i in flowing groundwater [$g\cdot m^{-3}$], $C_{i,im}$ the concentration of nuclide i in immobile porewater of rock matrix [$g\cdot m^{-3}$], D^* the apparent diffusion (or dispersion) coefficient in a fracture [$m^2\cdot sec^{-1}$], v the velocity of groundwater [$m\cdot sec^{-1}$], λ the decay constant [sec^{-1}], n_p the stoichiometric coefficient for the decay of parent nuclides [-], R the retardation coefficient [-], q_i the source/sink term by rock matrix diffusion [$g\cdot m^{-3}\text{-}sec^{-1}$], D the diffusion coefficient in the porewater rock matrix [$m^2\cdot sec^{-1}$], and ε the porosity of rock [-].

$$\begin{aligned} \frac{\partial C_i}{\partial t} &= D^* \frac{d^2 C_i}{d\chi^2} - v\frac{dC_i}{d\chi} - \lambda_i C_i + \sum_p n_p \lambda_p C_p + q_i \\ \frac{\partial C_{i,im}}{\partial t} &= \frac{D}{R}\frac{d^2 C_{i,im}}{dz^2} - \lambda_i C_{i,im} + \sum_p n_p \lambda_p C_{p,im} \\ q_i &= -\varepsilon D \frac{dC_{i,im}}{dz}\Big|_{z=b} \end{aligned} \tag{2}$$

The flow rate in the fracture is defined by the cubic law [17] as expressed in Eq. 3, where Q is the Darcy flow rate [$m^3\cdot sec^{-1}$], K_f the hydraulic conductivity of fracture [$m\cdot sec^{-1}$], A_f the cross-sectional area of fracture [m^2], ∇h the hydraulic gradient [-], $2b$ the aperture of fracture [m], w the width of fracture [m], μ the viscosity of groundwater [Pa·sec], ρ the density of groundwater [$kg\cdot m^{-3}$], and g the gravitational acceleration [$m\cdot sec^{-2}$]. In other words, the velocity of groundwater in the fracture is determined by its aperture. For the fracture intersecting the tunnel, an aperture of 10^{-5} m, which falls into a transmissivity in order of 10^{-10} $m^2\cdot sec^{-1}$, is assumed. The aperture of MWCF is assumed to be five times larger.

$$\begin{aligned} Q &= -K_f A_f \nabla h = -\frac{(2b)^3 w}{12\mu}\rho g \nabla h \\ v &= -K_f \nabla h = -\frac{(2b)^2}{12\mu}\rho g \nabla h \end{aligned} \tag{3}$$

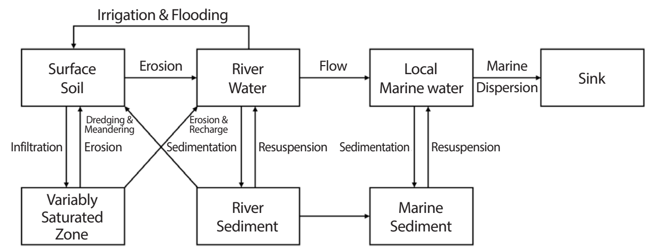

Fig. 3. The conceptual model for nuclides transport in biosphere compartment model (redrawn from [23]).

The released radionuclides migrate into a biosphere consisting of farming, riverside, and marine compartment (Fig. 3). The developed model can consider three exposure groups including farmer, riverside fisher, and marine fisher. The radiological exposure pathways are ingestion, inhalation, and external dose. Details on the concept of the biosphere are referred to elsewhere [23].

2.3 Computational Model

There are two series of system-level models developed in the KAERI: the Total System Performance Assessment model using GoldSim (GSTSPA) [24], and the KAERI's Performance Assessment Model (K-PAM) [9]. They are

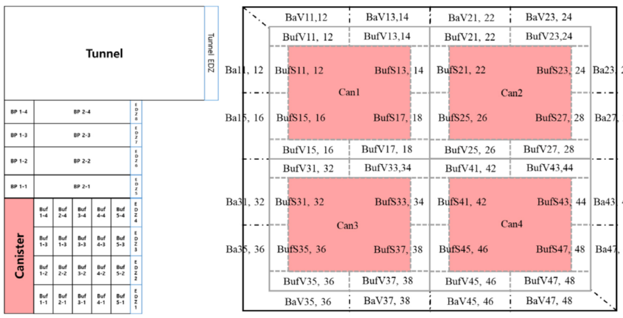

Fig. 4. Schematic diagram of cell network in EBS compartment model for KRS+: (left) PWR; (right) CANDU.

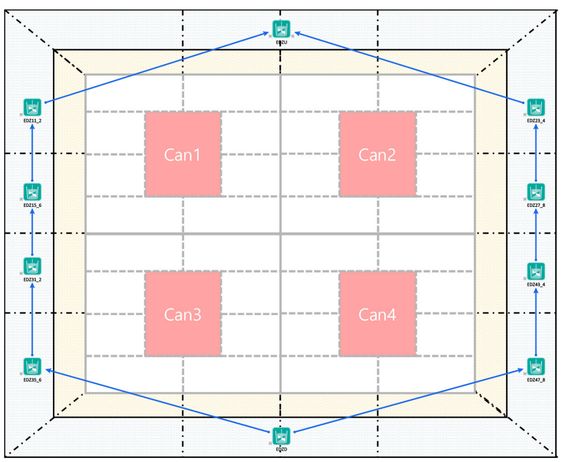

Fig. 5. Advection-diffusion transport pathway for EDZ of CANDU-H type repository.

both based on the GoldSim software, a simulation tool based on the compartment modeling approach [5]. The compartment modeling approach in the GoldSim assumes homogeneity in each compartment and calculates mass transfer among compartments based on their properties. Applying this modeling approach, the complexity of detailed processes in an extensive system of interest is avoided while the system's behavior can be expressed properly in a recognizable manner [4].

The GSTSPA is the first version model in KAERI to simulate radionuclides transport in disposal systems for various radioactive wastes and SNFs in a deterministic way. The next version model, the K-PAM, improved the GSTSPA to make probabilistic risk assessment possible. The probabilistic assessment enables the model to consider not only a single representative scenario but also complex scenarios. In this study, we modified the previous models by adding new evaluation options to evaluate the performance of the KRS+ design and the properties of the host rock, as presented in Section 2.2.

The modified model used in this study consists of four parts: the EBS, the fractured geosphere, the MWCF, and the biosphere. A cell pathway network calculates diffusive mass transport in the EBS model. Figure 4 shows the compartment model for the EBS of KRS+. In the EBS model, an excavated disturbed zone (EDZ) is coupled with a diffusive mass transfer link with the backfill and the buffer. Within the EDZ, advective flow is defined as described in the conceptual model (Fig. 5). To simulate mass transport through a fracture, a pipe pathway in the Goldsim transport module is used. The mass transport in the pipe pathway is calculated by numerical inverse Laplace transform of the solution for the basic governing equation given by Eq. 2. The details on Goldsim's numerical approach to calculate mass transfer in pipe pathway using the Eq. 2 are referred elsewhere [5].

3. Input Parameters for the Assessment

In this study's assessment scenario, the total amounts of SNFs to be disposed of are 62,420 assemblies of PLUS7 SNFs and 664,605 bundles of CANDU SNFs. The amount of each type of SNF is determined based on the 8th Basic Plan for Electric Power Demand and Supply [22]. The calculated numbers of disposal canister for PWR-V and CANDU-H type repository are 15,625 and 11,077, respectively. Three types of radionuclides inventory are considered: UO_2 matrix bounded inventory, structural material bounded inventory, and IRF inventory. The structural materials are fuel assembly of PWR, and cladding of CANDU. The values for bounded radionuclides inventory are summarized in Table 1 and Table 2.

Table 1. Radionuclides inventory for PWR and CANDU SNF

Radionuclides	PWR [g/canister]	CANDU [g/basket]	Radionuclides	PWR [g/canister]	CANDU [g/basket]
^{227}Ac	7.74×10^{-7}	4.24×10^{-8}	^{241}Pu	3.59×10^{2}	5.54×10^{1}
^{241}Am	2.77×10^{3}	3.18×10^{2}	^{242}Pu	1.74×10^{3}	1.08×10^{2}
^{243}Am	5.10×10^{2}	5.03×10^{0}	^{226}Ra	1.15×10^{-5}	1.19×10^{-6}
^{14}C	1.22×10^{0}	1.57×10^{-1}	^{228}Ra	5.07×10^{-12}	4.16×10^{-13}
^{36}Cl	7.51×10^{-1}	4.67×10^{-1}	^{222}Rn	7.39×10^{-11}	7.65×10^{-12}
^{245}Cm	1.17×10^{1}	2.35×10^{-3}	^{79}Se	1.32×10^{1}	1.74×10^{0}
^{246}Cm	1.58×10^{0}	2.58×10^{-4}	^{151}Sm	2.68×10^{1}	2.79×10^{0}
^{135}Cs	1.16×10^{3}	4.53×10^{1}	^{126}Sn	5.39×10^{1}	7.90×10^{0}
^{137}Cs	1.22×10^{3}	1.76×10^{2}	^{90}Sr	4.83×10^{2}	6.88×10^{1}
^{129}I	4.38×10^{2}	6.77×10^{1}	^{99}Tc	2.15×10^{3}	2.99×10^{2}
^{94}Nb	9.89×10^{1}	2.06×10^{-4}	^{229}Th	6.79×10^{-6}	6.84×10^{-8}
^{59}Ni	1.58×10^{2}	1.91×10^{-1}	^{230}Th	5.73×10^{-2}	6.52×10^{-3}
^{63}Ni	2.23×10^{1}	2.72×10^{-2}	^{232}Th	1.53×10^{-2}	1.30×10^{-3}
^{237}Np	1.57×10^{3}	5.61×10^{1}	^{233}U	2.66×10^{-2}	7.12×10^{-4}
^{231}Pa	1.75×10^{-3}	1.34×10^{-4}	^{234}U	5.31×10^{2}	5.85×10^{1}
^{107}Pd	6.67×10^{2}	8.77×10^{1}	^{235}U	1.21×10^{4}	2.85×10^{3}
^{238}Pu	5.11×10^{2}	5.57×10^{0}	^{236}U	1.10×10^{4}	1.10×10^{3}
^{239}Pu	1.05×10^{4}	3.67×10^{3}	^{238}U	1.58×10^{6}	1.39×10^{6}
^{240}Pu	5.26×10^{3}	1.53×10^{3}	^{93}Zr	2.11×10^{3}	1.62×10^{2}

Table 2. Radionuclides inventory for structural material

Radionuclides	PWR [g/canister]	CANDU [g/basket]
^{14}C	7.80×10^{-1}	4.31×10^{-2}
^{36}Cl	3.22×10^{-5}	2.40×10^{-6}
^{135}Cs	6.92×10^{-19}	1.33×10^{-25}
^{137}Cs	1.54×10^{-24}	3.26×10^{-32}
^{129}I	1.94×10^{-9}	9.15×10^{-14}
^{94}Nb	9.89×10^{1}	5.06×10^{-11}
^{59}Ni	1.58×10^{2}	1.68×10^{-2}
^{63}Ni	2.30×10^{1}	2.42×10^{-3}
^{107}Pd	7.63×10^{-12}	3.53×10^{-17}
^{79}Se	7.71×10^{-32}	0.00×10^{0}
^{90}Sr	1.91×10^{-5}	4.18×10^{-7}
^{99}Tc	1.76×10^{0}	7.22×10^{-7}
^{93}Zr	1.38×10^{2}	1.74×10^{1}

Table 3. Instantaneous release fraction (IRF) for SNF inventory in this study

Radionuclides	PWR*	CANDU**
^{14}C	0.11	0.027
^{36}Cl	0.13	0.060
^{135}Cs	0.043	0.040
^{137}Cs	0.043	0.040
^{129}I	0.043	0.040
^{79}Se	0.0065	0.006
^{90}Sr	-	0.025
^{99}Tc	-	0.010

* referred to [18].
** referred to [11].

Table 4. Distribution coefficient of nuclides in various mediums [$m^3 \cdot kg^{-1}$]

Elements	Buffer Dense Backfill	Backfill	Rock
Ac*	5.20×10^{0}	5.20×10^{0}	1.50×10^{-2}
Am*	2.50×10^{1}	2.50×10^{1}	1.50×10^{-2}
C**	2.70×10^{-2}	8.10×10^{-3}	0.00×10^{0}
Cl*	0.00×10^{0}	0.00×10^{0}	0.00×10^{0}
Cm*	2.50×10^{1}	2.50×10^{1}	1.50×10^{-2}
Cs*	3.10×10^{-2}	3.10×10^{-2}	3.50×10^{-2}
I*	0.00×10^{0}	0.00×10^{0}	0.00×10^{0}
Nb*	3.10×10^{0}	3.10×10^{0}	2.00×10^{-2}
Ni*	6.60×10^{-2}	6.60×10^{-2}	1.10×10^{-3}
Np*	3.90×10^{1}	3.90×10^{1}	5.30×10^{-2}
Pa*	3.10×10^{0}	3.10×10^{0}	5.90×10^{-2}
Pd*	5.10×10^{0}	5.10×10^{0}	5.20×10^{-2}
Pu*	3.90×10^{1}	3.90×10^{1}	1.50×10^{-2}
Ra*	1.10×10^{-3}	1.10×10^{-3}	2.40×10^{-4}
Rn*	0.00×10^{0}	0.00×10^{0}	3.00×10^{-4}
Se*	0.00×10^{0}	0.00×10^{0}	3.00×10^{-4}
Sm*	5.20×10^{0}	5.20×10^{0}	1.50×10^{-2}
Sn*	3.90×10^{1}	3.90×10^{1}	1.60×10^{-1}
Sr*	1.10×10^{-3}	1.10×10^{-3}	3.40×10^{-6}
Tc*	3.90×10^{1}	3.90×10^{1}	5.30×10^{-2}
Th*	3.90×10^{1}	3.90×10^{1}	5.30×10^{-2}
U*	3.90×10^{1}	3.90×10^{1}	5.30×10^{-2}
Zr*	4.70×10^{0}	4.70×10^{0}	2.10×10^{-2}

* Referred from [21].
** Referred from [3].

The model assumes that total canisters in the repository will fail at 10,000 years after the repository closure. Initial defects of canisters are not considered. For conservatism, a mechanism for waste matrix degradation is assumed to be fixed fractional dissolution rather than solubility limited congruent dissolution. The dissolution rates for waste matrixes are 10^{-7} fraction/year for SNF UO_2 matrix, and 10^{-4} fraction/year for SNF structural material [20]. The amount of gaseous fission product in the gap (IRF inventory) has not been evaluated in Korea yet so that data from foreign investigations are used and summarized in Table 3.

Table 5. Solubility limits of nuclides [$mol \cdot m^{-3}$] [3]

Elements	Solubility limit	Elements	Solubility limit
Ac	1.00×10^{-4}	Pu	1.00×10^{-6}
Am	1.00×10^{-4}	Ra	1.00×10^{-3}
C	1.00×10^{0}	Rn	-1.00×10^{0}
Cl	-1.00×10^{0}	Se	1.00×10^{-4}
Cm	1.00×10^{-4}	Sm	1.00×10^{-4}
Cs	-1.00×10^{0}	Sn	5.00×10^{-4}
I	-1.00×10^{0}	Sr	1.00×10^{1}
Nb	1.00×10^{-4}	Tc	1.00×10^{-5}
Ni	1.00×10^{-4}	Th	5.00×10^{-5}
Np	2.00×10^{-5}	U	5.00×10^{-5}
Pa	5.00×10^{-5}	Zr	1.00×10^{-5}
Pd	1.00×10^{-5}		

*No solubility limit.

Radionuclides database, including solubility limits and distribution coefficients in the repository system, are dependent on a chemical condition of groundwater. In a geologic repository system, groundwater is generally expected to have negative Eh and pH around 7~10 [3, 16, 18]. In this geochemical condition, radionuclides tend to have low mobility. For example, the dominating aqueous speciation of technetium under the anticipated geochemical condition in the repository is $TcO(OH)_2(aq)$ rather than highly mobile Tc(VII) forms [16, 18]. There are a few exceptions, however, including iodine, cesium, chlorine, Etc. Many countries have developed a database that is compatible with their geochemical condition. In the ROK, the KAERI has developed the radionuclides database based on the geochemical condition in KAERI Underground Research Tunnel (KURT) [3]. Accordingly, solubility data in the condition of the KURT are used in this study. Distribution coefficients, on the other hand, are referred from SR-Site study in Sweden because the values of KAERI are under review [19]. The radionuclides database used in this study is summarized in Table 4 and Table 5.

4. Results and Discussion

4.1 Major Radionuclides Contributing Radiological Impact

Figure 6 shows an annual radiological dose to a representative group from the KRS$^+$ disposal system: total SNF inventory from PWR and CANDU is postulated. Here, the representative group means farmers because other groups' impacts are not as significant as farmers'. Among many radionuclides included in the SNF inventory, radionuclides, which meaningfully affect the radiological exposure dose, are long-lived fission products (^{129}I, ^{36}Cl, ^{135}Cs), activation product (^{14}C), and decay product from ^{238}U (^{226}Ra). These radionuclides have high mobility in the geosphere of the disposal system. The peak dose rate is 8.19×10^{-4} mSv·yr^{-1} and is mostly attributed to ^{129}I near after the failure of disposal canisters. A dose limit criterion for low and intermediate level wastes repository in Korea is 0.1 mSv·yr^{-1}. Therefore, the KRS$^+$ design shows a sufficient safety margin despite the conservative assumptions made in the natural barrier.

Readers should be noted that radiological dose contributions from transuranic elements and uranium are not observed in the results. The low radiological impact of the heavy elements in disposal systems is also found in various references [10, 14, 19] and is attributed to their low mobility reducing groundwater condition. The mobility of radionuclides can be understood in terms of distribution coefficient and solubility. The distribution coefficient of radionuclide (K_d) in a geological medium is defined as Eq. 4, where S is the concentration in the solid medium [g·kg^{-1}], and C is the concentration in groundwater [g·m^{-3}]. The high distribution coefficient implies that the radionuclide tends to stay in the solid medium rather than migrate through the groundwater flow.

Peak radiological doses and peak time of each significant radionuclides are shown in Table 6. Considering the distribution coefficients in Table 4, the results show that the smaller a distribution coefficient is, the shorter the peak time is except for ^{226}Ra. The peak time means a traveling time for a radionuclide to reach the biosphere after it starts to release. In other words, the apparent transport velocity of a radionuclide with high distribution coefficient is slow due to sorption into the rock matrix. The exception for the long traveling time of ^{226}Ra is due to the significantly low mobility of its mother nuclide: ^{226}Ra is a decay product of ^{238}U.

$$K_{d,i} \equiv S/C \tag{4}$$

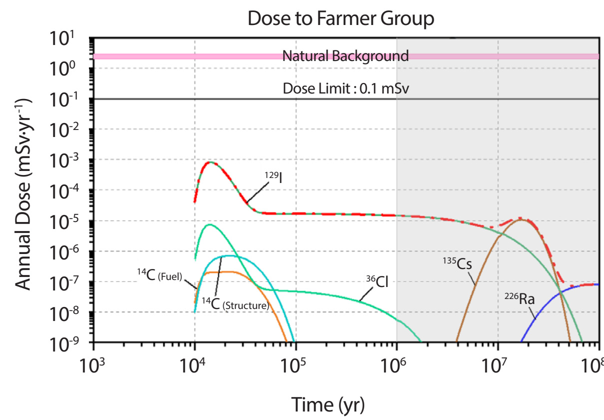

Fig. 6. Radiological exposure dose to farmer group by the KRS$^+$ with disposed PWR and CANDU SNFs: fixed fractional dissolution for fuel and structural inventory.

Table 6. Peak radiological doses and times of the major nuclides in the result

Nuclides	Peak dose rate (mSv·yr^{-1})	Peak time (yr)
^{129}I	8.19×10^{-4}	14,000
^{36}Cl	7.33×10^{-6}	14,000
^{14}C	9.05×10^{-7}	22,000
^{135}Cs	1.06×10^{-5}	17,000,000
^{226}Ra	7.99×10^{-8}	> 100,000,000

4.2 Contribution by Source Terms

Three source terms considered in this study are radionuclides in spent fuel rod (UO_2 bounded inventory), gap (IRF inventory), and structural material. A final radiological impact of each source term is determined by the dissolution or the

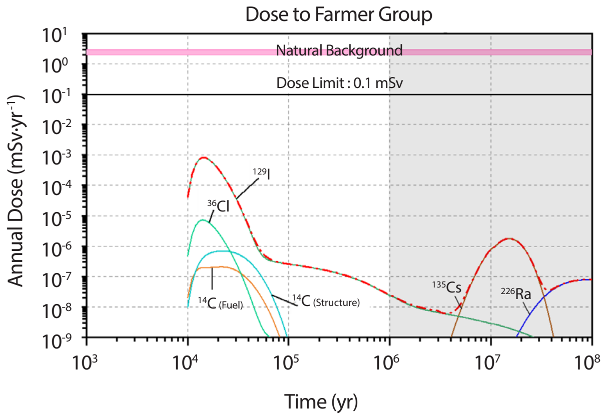

Fig. 7. Radiological exposure dose to farmers by the KRS+: congruent dissolution for fuel inventory and fixed fractional dissolution for structural inventory.

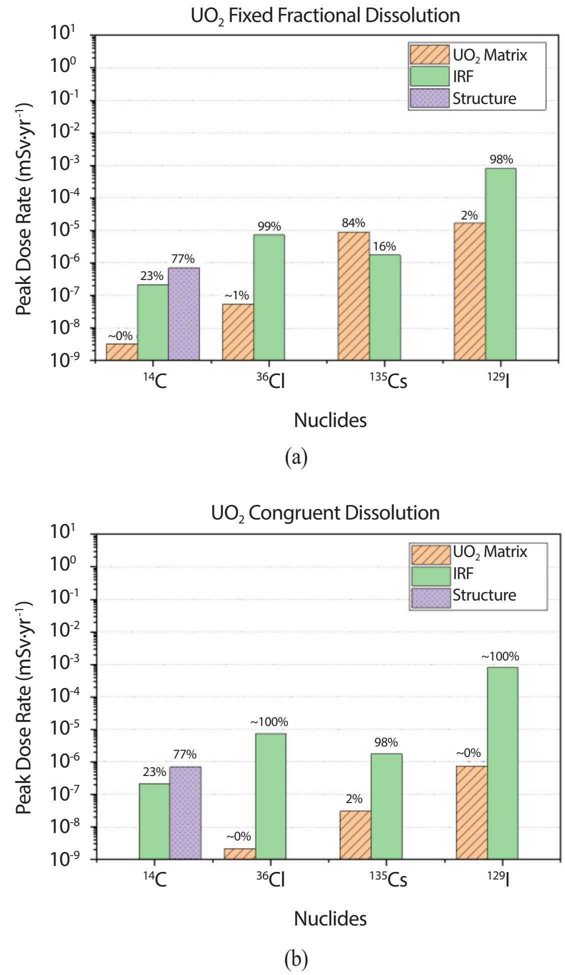

Fig. 8. The peak dose rates of major radionuclides by three source terms: (a) fixed fractional dissolution of UO_2 matrix; (b) solubility limited congruent dissolution of UO_2 matrix.

degradation rate of its waste matrix. For example, most of the spent fuel rod is composed of UO_2 so that radionuclides in the UO_2 matrix cannot be exposed to groundwater until the surrounding matrix is degraded.

As mentioned in Section 3, the dissolution of UO_2 and structural material is calculated by the fixed fractional dissolution rate. In other words, the model assumes that a specified fraction of radionuclides is exposed to and is dissolved into groundwater in a year. This calculation method is quite a conservative assumption for the UO_2 matrix because UO_2 is a very stable solid phase in reducing groundwater conditions. The more realistic mechanism for fuel degradation would be solubility limited congruent dissolution. Figure 7 shows the result when the model uses the congruent dissolution option for the spent fuel matrix. In Fig. 7, the plateau of ^{129}I after its first peaks in Fig. 6 is not present while the peak value is not changed: the peak of ^{129}I is mainly attributed to IRF inventory. This tendency is also the same for ^{36}Cl. In the case of ^{135}Cs, whose curve shows no plateaus in Fig. 6, the peak doses are reduced when congruent dissolution is assumed. Putting together these results, it means that in a realistic simulation, most of the radionuclides within the spent fuel matrix will stay immobile until they decay.

Figure 8 shows the peak dose rate of each major radionuclides given by the three different source terms when the fixed dissolution rate is assumed. The radiological impacts of all significant radionuclides except ^{14}C and ^{137}Cs are mainly attributed to the IRF inventory. This tendency is the same when the congruent dissolution of the spent fuel matrix is assumed; thereby, the most significant radiological peak is determined by the IRF unless the waste matrix is unstable. Considering that the IRFs used in this study are referred from foreign data, the characterization IRF of Korean SNF will be significant in the future. A considerable amount of ^{14}C and ^{135}Cs, however, comes from fuel and structure inventory. In the case of ^{14}C, the reason for this

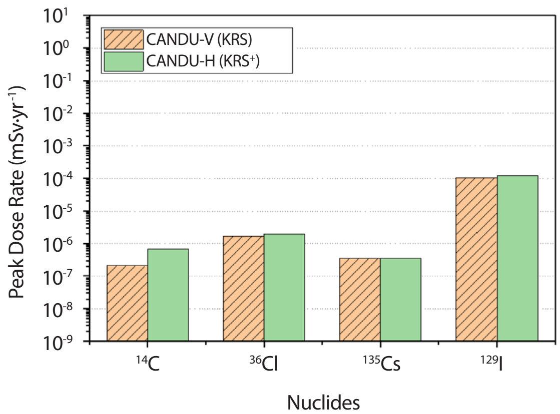

Fig. 9. Comparison on the peak dose rates of major nuclides for CANDU between the KRS and KRS+ (fixed fraction dissolution rate is assumed).

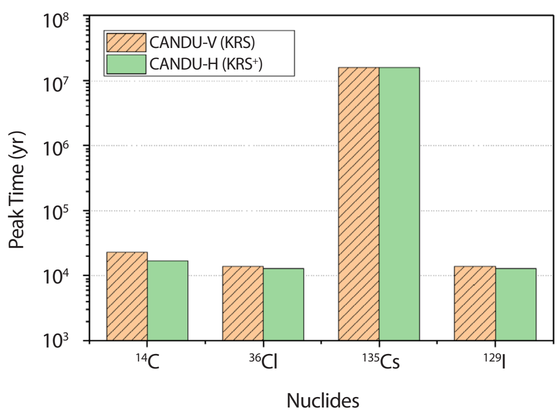

Fig. 10. Comparison on the peak times of major nuclides for CANDU between the KRS and KRS+ (fixed fraction dissolution rate is assumed).

tendency is due to poor matrix stability of structure material: the fixed dissolution rate of 10^{-4} fraction/yr is applied to structural material. Uncertainty in the potential impact of structure material has not been investigated in detail yet so that future studies will be required. The peak of ^{135}Cs is mainly contributed to the fuel matrix inventory. However, we do not consider ^{135}Cs as a future problem based on three reasons: the peak time is beyond the scope of the safety assessment period (one million years); the peak is small enough compared with ^{129}I; fairly stable characteristic of the UO_2 matrix will effectively suppress the release of Cs in the long-term.

4.3 Comparison between KRS and KRS$^+$: CANDU-V and CANDU-H

The essential improvement of the KRS$^+$ from the KRS is disposal efficiency in a repository area. This improvement is especially evident for the repository design for CANDU SNFs by disposing of them in the horizontal two layers repository (CANDU-H of KRS$^+$) rather than in the vertical borehole (CANDU-V of KRS) [8]. To confirm that the KRS$^+$ EBS for CANDU is still enough, safety assessments for the two different concepts are conducted. As Fig. 9 and Fig. 10 show, all radionuclides' peak dose rates slightly increase while the peak times decrease. These two differences imply that the diffusion length of the CANDU-H is shorter than the one of CANDU-V. However, the difference between these two designs is not significant so that the performance of CANDU-H is sufficient.

5. Conclusion

Safety assessment of a radioactive waste repository is a platform for the evolutionary design process required to accomplish a complete disposal project. In this context, this paper introduces the system-level insight model to evaluate the transport of radionuclides in a disposal system based on the KRS$^+$ design. In addition, preliminary safety assessment results based on the model are also provided. The peak dose rate to representative exposure groups shows that the EBS of the KRS$^+$ design can secure the safety margin at least in order of two until the EBS performance maintains. When it comes to the average natural background radiological dose of 2~3 mSv·yr^{-1}, the safety margin falls into an order of three. ^{129}I is evaluated to be the most critical radionuclide due to its long half-life and high mobility. Other key radionuclides showing considerable impacts in the period of safety assessment are ^{36}Cl, ^{14}C. The significant contribution of ^{129}I and ^{36}Cl comes from the IRF inventory, while the contribution of ^{14}C comes from both the IRF and structure material inventory. Based on this result, a detailed study on these two inventories would be necessary in the future.

The EBS of the KRS$^+$ is the one part where lots of improvements have been made. Significantly, the footprint area of the CANDU repository is reduced. Despite the reduced area, it is evaluated that the performance of the KRS$^+$ EBS for CANDU is similar to the previous design. Nonetheless, the KRS$^+$ design needs to be detailed and modified, considering various geologic conditions of potential sites. This requirement is because a designation of the disposal site hosting an un-preferred geologic characteristic is possible due to the distinct socio-geographical environment in Korea. Like the Structured Approach of NUMO, the KRS$^+$ design will be tailored to potential repository sites. This study will provide the reference repository design for SNF in Korea as a starting point of this plan.

Acknowledgement

This work was supported by the Ministry of Science and ICT within the framework of the national long-term nuclear R&D program (NRF-2017M2A8A5014856).

REFERENCES

[1] C.H. Kang, J.W. Choi, W.I. Ko, Y.M. Lee, J.H. Park, Y.S. Hwang, and S.K. Kim. Reference Spent Fuel and Its Characterstics for the Concept Develpment of a Deep Geologcial Disposal System, Korea Atomic Energy Research Institute Report, KAERI/TR-914/97 (1997).

[2] D.K. Cho, J. Kim, I.Y. Kim, and J.-Y. Lee, “Investigation of PWR Spent Fuels for the Design of a Deep Geological Repository”, J. Nucl. Fuel Cycle Waste Technol., 17(3), 339-346 (2019).

[3] D.K. Cho, N.Y. Ko, Y.K. Koh, J.S. Kwon, I.Y. Kim, J.W. Kim, J.H. Ryu, K.W. Park, C.K. Park, T.J. Park, M.H. Baik, S. Yoon, M. Lee, S.Y. Lee, J.K. Lee, J.O. Lee, J. Lee, C. Lee, S. Jung, J. Jeong, and S.-H. Ji. A Safety Case of the Conceptual Disposal System for Pyroprocessing High-Level Waste Based on the KURT Site (AKRS-16): VI. Model and Data”, Korea Atomic Energy Research Institute Report, KAERI/TR-6732/2016 (2016).

[4] E. Eriksson, “Compartment Models and Reservoir Theory”, Annu. Rev. Ecol. Syst., 2, 67-84 (1971).

[5] GoldSim Technology Group LLC. GoldSim Contaminant Transport Module. Issaquah, Washington: GoldSim Technology Group LLC (2018).

[6] H. Ju and I.-S. Hwang, “Systematic model for estimation of future inadvertent human intrusion into deep rad-waste repository by domestic groundwater well drilling”, Nucl. Eng. Des., 327, 38-50 (2018).

[7] I.-Y. Kim, D.-K. Cho, and H.-J. Choi, Analysis on Characteristics of Reference SNF for KRS$^+$ Design - I. PLUS7 SNF. (2019).

[8] J. Lee, I.-Y. Kim, H. Ju, H.-J. Choi, and D.-K. Cho, “Proposal of an Improved Concept Design for the Deep Geological Disposal System of Spent Nuclear Fuel in Korea”, J. Nucl. Fuel Cycle Waste Technol., 18(S), 1-19 (2020).

[9] J.W. Kim, D.K. Cho, N.Y. Ko, J. Jeong, and M.H. Baik, “Model Development for Risk-based Safety Assessment of a Geological Disposal System of Radioactive Wastes Generated by Pyro-processing of PWR Spent Fuel in Korea”, Nucl. Technol., 203(1), 1-16 (2018).

[10] K.-S. Kim, C.-H. Kang, N.-Y. Ko, Y.-K. Koh, J.-S. Kwon, G.Y. Kim, I.-Y. Kim, J.-W. Kim, J.S. Kim, J.-H. Ryu, K.W. Park, C.-K. Park, T.-J. Park, D.-S. Bae, M.-H. Baik, S. Yoon, M. Lee, S.Y. Lee, Y.-M. Lee, J.-K. Lee, J.O. Lee, J. Lee, J. Lee, C. Lee, S. Jung, J. Jeong, D.-K. Cho, W.-J. Cho, S.-H. Ji, Y.-C. Choi, H.-J. Choi, and P.-S. Hahn. A Safety Case of the Conceptual Disposal System for Pyro-processing High-Level Waste Based on the KURT Site (AKRS-16): Safety Case Synthesis Report, Korea Atomic Energy Research Institute Report, KAERI/TR-6726/2016 (2016).

[11] M. Gobien, F. Garisto, E. Kremer, and C. Medri. Sixth Case Study: reference Data and Codes, Nuclear Waste Management Organization Report, NWMO-TR-2016-10 (2016).

[12] Nuclear Waste Management Organization of Japan. Development of Repository Concepts for Volunteer Siting Environment, NWMO Report, NUMO-TR-04-03 (2004).

[13] Nuclear Waste Management Organization of Japan. The NUMO Structured Approach to HLW Disposal in Japan: Staged Project Implementation at Volunteer Sites Utilising a Requirements Management System, NWMO Report, NUMO-TR-07-02 (2007).

[14] Posiva Oy. Safety Case for the Disposal of Spent Nuclear Fuel at Olkiluoto - Assessment of Radionuclie Release Scenarios for the Repository System 2012, POSIVA Oy Report, POSIVA 2012-09 (2012).

[15] Posiva Oy. Safety Case for the Disposal of Spent Nuclear Fuel at Olkiluoto - Design Basis 2012, POSIVA Oy Report, Posiva 2012-03 (2012).

[16] Posiva Oy. Safety Case for the Disposal of Spent Nuclear Fuel at Olkiluoto: Radionuclide Solubility Limits and Migration Parameters for the Backfill, POSIVA Oy Report, POSIVA 2012-40 (2012).

[17] R.W. Zimmerman and G.S. Bodvarsson. Hydraulic Conductivity of Rock Fractures, University of California Report, LBL-35976 (1994).

[18] Svensk Kärnbränslehantering AB. Data report for the safety assessment SR-Site, SKB Technical Report, SKB-TR-10-52 (2010).

[19] Svensk Kärnbränslehantering AB. Design and production of the KBS-3 repository, SKB Technical Report, SKB-TR-10-12 (2010).

[20] Svensk Kärnbränslehantering AB. Fuel and canister process report for the safety assessment SR-Site, SKB Technical Report, SKB-TR-10-46 (2010).

[21] Svensk Kärnbränslehantering AB. Radionuclide transport report for the safety assessment SR-Site, SKB Technical Report, SKB-TR-10-50 (2010).

[22] Ministry of Trade, Industry, and Energy. The 8th Basic Plan for Long-term Electricity Supply and Demand (2017-2031), MOTIE Notice No.2017-611 (2017).

[23] Y. Hwang, S.-G. Kim, and C.-H. Kang. Assessment on the Biophsere of a Potential HLW Repository in Korea, Korea Atomic Energy Research Institute Report, KAERI/TR-2308/2002 (2002).

[24] Y.-M. Lee and Y. Hwang. A GoldSim Model and a Sensitivity Study for Safety Assessment of a Repository for Disposal of Spent Nuclear Fuel, Korea Atomic Energy Research Institute Report, KAERI/TR-3660/2008 (2008).